High-Resolution Steady State Magnetic Resonance Angiography of the Carotid Arteries: Are Intravascular Agents Necessary?

Feasibility and Preliminary Experience With Gadobenate Dimeglumine

Michele Anzidei, MD, Alessandro Napoli, MD,* Beatrice Cavallo Marincola, MD,* Miles A. Kirchin, PhD,† Cristina Neira, PhD,‡ Daniel Geiger, MD,* Fulvio Zaccagna, MD,* Carlo Catalano, MD,* and Roberto Passariello, MD**

Purpose: To prospectively evaluate the potential of gadobenate dimeglumine for high-resolution steady-state (SS) contrast-enhanced magnetic resonance angiography (CE-MRA) of the carotid arteries as an adjunct to conventional first-pass (FP) MRA, with computed tomography angiography (CTA) and digital subtraction angiography (DSA) as reference.

Materials and Methods: Institutional ethics committee approval and written informed consent were obtained. Forty consecutive patients underwent conventional FP MRA with 15 mL gadobenate dimeglumine, using a conventional 3D FLASH sequence (14 sec acquisition time). Immediately afterward, SS images were obtained using a high resolution coronal 3D FLASH sequence (240 sec acquisition time). All patients also underwent CTA and conventional DSA within 8 ± 3 days. Three experienced radiologists assessed FP and SS image quality and calculated sensitivity, specificity, accuracy, and predictive values for stenosis grade and length, plaque morphology, and tandem lesions using DSA as reference. Detected stenoses were quantified and compared (Spearman rank correlation coefficient, [R(s)]; McNemar test) with DSA and CTA findings. Inter-read variability was assessed using kappa (κ) statistics. The impact of SS acquisitions on diagnostic confidence and patient management was assessed.

Results: MRA FP and SS image quality was excellent in 63 (78.8%) and 46 (57.5%) vessels, adequate in 11 (13.8%) and 20 (25.0%) vessels, and poor in 6 (7.5%) and 14 (17.5%) vessels, respectively. Area under the curve analysis revealed no significant differences between MRA FP, MRA FP + SS, and CTA for the grading of stenoses ($P = 0.838$; accuracy values of 97.4%, 97.4%, and 98.7%, respectively). Greater accuracy ($P < 0.001$) was noted for FP + SS images over FP images alone for the assessment of plaque morphology (96.1% for FP + SS images vs. 83.3% for FP). Increased diagnostic confidence was noted for 49 (61.3%) vessels because of additional SS images whereas an impact on final diagnosis was noted in 8 (10%) cases. Good correlation was noted between SS image quality and impact on final diagnosis (R(s) = 0.7; $P < 0.0001$).

Conclusion: SS imaging of the carotid arteries is feasible with gadobenate dimeglumine. The increased spatial resolution attainable allows improved evaluation of stenoses and plaque irregularity, yielding comparable diagnostic performance to that of CTA and DSA.

Key Words: contrast-enhanced MR angiography, carotid arteries, vascular disease, gadobenate dimeglumine, intravascular contrast enhancement

(*Invest Radiol* 2009;44: 784–792)

A recent meta-analysis of the noninvasive tests available for imaging the carotid arteries has determined that contrast-enhanced magnetic resonance angiography (CE-MRA) is the most accurate for detection of significant (70%–99%) symptomatic stenosis.[1] With the availability of dedicated "blood pool" contrast agents that possess extended intravascular residence times, the conventional CE-MRA technique involving image acquisition during the first pass (FP) of a gadolinium-based contrast agent through the vessel of interest can potentially be extended to include also steady-state (SS) image acquisition in which images with increased spatial (isotropic) resolution are acquired without temporal constraints during the equilibrium phase of contrast circulation after the initial FP.[2–4] However, whereas dedicated intravascular agents offer the potential for additional diagnostic information and can be of immediate value in patients whose initial FP examination has failed for technical reasons (eg, bolus mistiming) or otherwise proven nondiagnostic, they are relatively costly and of limited diagnostic value for applications other than CE-MRA applications. In light of these limitations, any means to obtain similar diagnostic information to that afforded by high-resolution SS images without having to use a dedicated intravascular agent may be of great clinical interest.

Gadobenate dimeglumine (MultiHance; Bracco Imaging SpA, Milan, Italy) is a gadolinium-based MR contrast agent which resembles the conventional FP gadolinium agents in terms of its pharmacokinetics,[5] physicochemical properties,[6] and safety profile,[7–10] but which differs in possessing increased R1 relaxivity in blood[11,12] because of weak, transient interactions of the Gd-BOPTA contrast-effective molecule with serum albumin.[13–16] Several studies have shown that gadobenate dimeglumine possesses preferential vascular imaging properties compared with conventional gadolinium agents that do not interact with serum proteins and which have standard R1 relaxivity.[17–22] Moreover, the diagnostic performance of FP gadobenate dimeglumine-enhanced MRA has previously been shown to be comparable to that of digital subtraction angiography (DSA) for detection of clinically relevant carotid artery stenosis.[23] As yet, however, no studies have been performed to determine the feasibility of SS image acquisition with gadobenate dimeglumine as a possible adjunct to conventional FP image acquisition and, if feasible, whether combined FP + SS image acquisition is of addi-

Received June 9, 2009, and accepted for publication, after revision, July 16, 2009.

From the *Department of Radiological Sciences, University of Rome "La Sapienza," Rome, Italy; †Bracco Imaging SpA, Worldwide Medical and Regulatory Affairs, Milan, Italy; and ‡CRB Bracco Imaging SpA, c/o Bioindustry Park Canavese, via Ribes 5, 10010 Colleretto Giacosa, Italy.

Miles A. Kirchin is an employee of Bracco Imaging SpA but did not take part in study planning, in data acquisition, or in the analysis/interpretation of study findings.

Cristina Neira is a fellow engineer at Bracco SpA funded by a national grant from the Italian government but did not take part in data acquisition or data analysis/interpretation.

For all other authors there is no potential conflict of interest that could be perceived to bias our work. Authors had full control of all the data and information presented in this manuscript. Written informed consent was obtained by all the patients involved in the study and the whole study protocol was approved by the local ethics committee.

Reprints: Carlo Catalano, MD, Department of Radiological Sciences, University of Rome "La Sapienza," Viale Regina Elena 324, 00161, Rome, Italy. E-mail: carlo.catalano@uniroma1.it.

ISSN: 0020-9996/09/4412-0784

tional value over FP imaging alone for the detection of clinically relevant vascular disease.

The aims of this study were firstly to determine whether SS imaging of the carotid arteries is feasible with gadobenate dimeglumine; second, to ascertain whether SS imaging with gadobenate dimeglumine provides additional diagnostic information compared with FP imaging alone, and, finally, to preliminarily evaluate the diagnostic performance of FP and FP + SS imaging with gadobenate dimeglumine compared with routine computed tomography angiography (CTA) using DSA as reference standard.

MATERIALS AND METHODS

Patient Population and Informed Consent

This study was approved by the local institutional ethics committee and all evaluated subjects provided written informed consent after being informed of the potential benefits and contraindications of CE-MRA, CTA, and DSA. No funding or assistance in the planning or conduct of this study or in the interpretation of study findings was received from any commercial organization.

Consecutive patients with symptomatic carotid artery stenosis and/or irregular/ulcerated plaque at preliminary Doppler ultrasonography were enrolled between June and December 2008. All patients were referred for preoperative vascular imaging by vascular surgeons or interventional radiologists. Subjects who presented general contraindications to CE-MRA, CTA, or DSA or who had previously undergone carotid endarterectomy or stenting were ineligible for enrollment. Clinical studies were performed in the order outlined below with MRA performed first, followed by CTA and finally DSA.

Serum creatinine levels (average ± SD) were measured in all patients before and at 48 to 72 hours after each CTA and DSA examination; Student's *t* test was used to test for statistically significant differences before and after each examination.

Contrast-Enhanced MRA

All CE-MRA examinations were performed on a 1.5 T MR scanner (Magnetom Avanto; Siemens Medical Systems, Erlangen, Germany) (gradient strength: 45 mT/m; maximum slew rate: 200 T/m/s) equipped with a neurovascular array head and neck coil.

Routine FP CE-MRA was performed in the coronal plane using a 3D spoiled gradient-echo (GRE) sequence optimized for high spatial resolution and short acquisition time (repetition time [TR]: 3.5 milliseconds, echo time [TE]: 1.2 milliseconds, flip angle [FA]: 30 degrees, slice thickness: 0.7 mm, matrix: 384 × 384, voxel size: 1.0 × 1.0 × 0.7 mm, average: 1, bandwidth 380 Hz/Px, IPAT ×2, acquisition time: 14 seconds). Contrast enhancement was achieved using a standard volume of 15 mL (0.1 mmol/kg bodyweight for a 75 kg person) of gadobenate dimeglumine (MultiHance; Bracco Imaging SpA, Milan, Italy) administered by automatic injection through a 20G intravenous catheter at a rate of 2 mL/s, followed by 15 mL of saline flush at the same rate. On a weight-adjusted basis the dose administered ranged between 0.09 and 0.11 mmol/kg bodyweight. The delay between contrast injection and FP image acquisition was determined by means of bolus-tracking (CARE bolus; Siemens Medical Systems).

Acquisition of SS images began immediately after the FP acquisition. A modified higher-resolution 3D spoiled GRE sequence (TR: 7.5 milliseconds, TE: 2.3 milliseconds, FA: 30 degrees, slice thickness: 0.7 mm, matrix: 512 × 512, voxel size: 0.7 × 0.7 × 0.7 mm, average: 2, bandwidth 130 Hz/Px, IPAT ×2, acquisition time: 240 seconds) was used.

CT Angiography

All examinations were performed on a 64-detector scanner (Somatom Sensation 64; Siemens Medical Solutions, Forchheim; Germany) with 32 × 2 detectors with z-flying focal spot technology and gantry rotation time of 0.33 seconds.

CTA was performed from the aortic arch to the intracranial circulation using 50 mL of Iomeprol 400 (Iomeron 400, 400 mgI/mL; Bracco Imaging SpA, Milan, Italy) followed by 40 mL of saline flush, administered at 4 mL/s using a dual-head power CT injector system (Medrad, Pittsburgh, PA) through a 18G intravenous catheter. The scanning parameters were as follows: 120 kV, 180 mAs, detector configuration; 64 × 0.6 mm; pitch, 0.8; slice thickness, 0.7 mm; reconstruction increment, 0.5 mm. Scan initiation was triggered manually 5 seconds after arrival of the contrast agent bolus (determined by bolus-tracking).

Digital Subtraction Angiography

DSA was performed in all patients after femoral artery catheterization (Easyvision; Philips, Best, The Netherlands). Arch aortograms were obtained using a 5F pigtail catheter and were followed by selective catheterization of the common carotid arteries using a 7F guiding catheter. Images of the bifurcations and intracranial circulation were obtained in anteroposterior, lateral, and oblique projections (+45 degrees and −45 degrees). A 20 mL volume of contrast medium (Iomeprol 300, Iomeron 300, 300 mgI/mL; Bracco Imaging SpA, Milan, Italy) injected at 20 mL/s (automatic injector) was used for the arch whereas 8 mL volumes injected at 6 mL/s (hand injection) were used for each carotid artery projection. A field-of-view of 33 × 40 cm was used with a 1024 × 1024 matrix giving an average spatial resolution of 0.32 × 0.32 mm.

Image Analysis

All CE-MRA datasets were evaluated for image quality by 3 experienced blinded readers (CC, AN, MA with 10, 6, and 5 years of experience, respectively). The quality of FP and SS images in terms of vessel enhancement and wall delineation was assessed subjectively using a 3-point scale (1, excellent [homogenous vessel enhancement, high intraluminal signal, precise wall delineation]; 2, adequate [homogenous vessel enhancement, sufficient intraluminal signal and wall delineation]; 3, poor [inhomogeneous vessel enhancement, poor intraluminal signal and wall delineation]). Additional independent factors potentially leading to reduced image quality (eg, motion artifacts; venous contamination on FP images; poor artery-vein differentiation on SS images) were considered.

The same 3 readers thereafter independently evaluated the CE-MRA and CTA datasets for the presence and degree of steno-occlusive disease. For MRA, the FP datasets were read first followed by the FP and SS images combined. All image sets were presented in randomized order with a minimum interval of 2 weeks between individual readings of MRA FP images, MRA FP + SS images, and CTA images to avoid recall bias.

Image evaluation was in all cases performed using maximum intensity projection (MIP) reconstructions to identify the site of stenosis and direct and centroluminal multiplanar reformations (MPR and c-MPR, respectively) to quantify the degree of stenosis. Source images were also available for assessment. Detected stenoses were graded according to the 5-point classification scheme of the North American Symptomatic Carotid Endarterectomy Trial: I (0%–29%), II (30%–49%), III (50%–69%), IV (70%–99%), or V (100%; occlusion).[24] When the criteria for near-occlusion were met vessels were excluded from stenosis degree calculations. In each case, a cut-off value of 70% indicated a clinically relevant stenosis.[24]

Plaques identified during each reading were defined as irregular if small superficial irregularities were evident, and as ulcerated if a deep niche with clear profiles was apparent. The length of a

given stenosis was assessed using a 3-point scale from 1 (<10 mm) through 2 (10–15 mm) to 3 (>15 mm). The presence/absence of tandem lesions was evaluated from the aortic arch to the intracranial vessels.

For MRA examinations alone, the 3 readers subjectively determined whether SS images had any beneficial diagnostic impact when combined with FP images. A 4-point qualitative scale from −1 to 2 was used as follows: −1, SS images are nondiagnostic; 0, SS images provide no additional benefit; 1, SS images enable increased confidence for final diagnosis; and 2, SS images positively impact the final diagnosis.

All determinations were based on concordant findings of the 3 readers. If one readers' interpretation differed from those of the other 2, the concordant agreement of the other 2 readers was considered final. If the interpretations of all 3 readers differed, the images in question were re-evaluated by the 3 readers in consensus.

Evaluation of DSA images was performed independently by a highly experienced vascular radiologist (with 15 years experience) using a 2 mega-pixel workstation (Barco NV; Kortrijk, Belgium) equipped with a digital measuring system.

Statistical Analysis

Statistical analysis was performed using STATA 8.1 software (Stata Corporation; College Station, TX). Inter-read agreement concerning the degree of stenosis, plaque morphology, stenosis length, and tandem lesions was determined using generalized kappa (κ) statistics. The same methodology was used for inter-reader assessment of MRA image quality. Agreement was defined as very good ($\kappa > 0.8$) good ($\kappa = 0.61$–0.8), moderate ($\kappa = 0.41$–0.6), fair ($\kappa = 0.21$–0.4), or poor ($\kappa \leq 0.2$).

Determination of diagnostic performance (accuracy, sensitivity, specificity, positive predictive value and negative predictive value) was performed for each imaging modality for degree of stenosis, plaque morphology, plaque length, and tandem lesions. Additional analysis was performed for MRA image sets with SS acquisitions rated as excellent or adequate (score 1 or 2) and poor (score 3) in terms of image quality. McNemar's test and receiver-operator curve analysis were performed to compare diagnostic performance between modalities. Differences in image quality between FP and SS images were assessed using Wilcoxon's rank test. Finally, Spearman's test was used to determine the correlation between the quality of SS images and their impact on final diagnosis.

RESULTS

A total of 40 consecutive patients (25 male, 15 female; mean age, 64.4 years ± 14.8 standard deviation; range, 26–87 years) were enrolled. CE-MRA, CTA, and DSA examinations were performed in all patients without complications. The average room time was 21 ± 2 minutes for MRA, 15 ± 2 minutes for CTA, and 40 ± 6 minutes for DSA. The mean time period required to complete the entire imaging protocol was 8 ± 3 days. A total of 80 carotid bifurcations were examined; the average review time for each examination was 5 ± 1 minute for MRA FP images, 9 ± 3 minutes for MRA FP + SS images, 6 ± 2 minutes for CTA images, and 4 ± 2 minutes for DSA images.

Serum creatinine levels before (1.003 ± 0.212, range: 0.49–1.28) and 48–72 hours after (1.008 ± 0.205, range: 0.55–1.3) iodinated contrast injection were not significantly different ($P = 0.203$).

Quality of CE-MRA Images

Inter-reader agreement was excellent for evaluations of MRA image quality ($0.90 < \kappa < 0.93$). The quality of FP images was considered excellent for 63 of 80 (78.8%) vessels, adequate for 11 of 80 (13.8%) vessels, and poor for 6 of 80 (7.5%) vessels. Similarly, the quality of SS images was considered excellent for 46 of 80 (57.5%) vessels, adequate for 20 of 80 (25%) vessels, and poor for 14 of 80 (17.5%) vessels. The 6 poor vessels at FP imaging (5 due to slight acquisition mistiming and 1 due to patient movement) were considered adequate at SS imaging whereas the 14 poor vessels at SS imaging (in all cases due to patient movement during the extended acquisition time) were all of adequate or excellent quality at FP imaging. Significantly ($P < 0.001$; Wilcoxon rank test) higher overall image quality was achieved for FP images compared with SS images.

Grading of Stenoses

Agreement between readings was good to very good ($0.72 < \kappa < 0.86$) regarding the grading of stenosis. Values for accuracy, sensitivity, specificity, positive predictive value, and negative predictive value are given in Table 1. Two stenoses were rated as "near occlusion" on all images and were excluded from subsequent determinations of diagnostic performance. For cases in which SS image quality was poor the accuracy of the FP reading alone was higher than that of the combined FP + SS reading (14/14 [100%] vs. 13/14

TABLE 1. Diagnostic Performance of FP MRA, FP + SS MRA, and CTA for the Grading of Carotid Artery Stenosis

		SS Image Quality		
Parameter	Image Set	All (n = 78)	Adequate/ Excellent (n = 64)	Poor (n = 14)
Accuracy	FP MRA	97.4% (76/78)	96.9% (62/64)	100% (14/14)
	FP + SS MRA	97.4% (76/78)	98.4% (63/64)	92.8% (13/14)
	CTA	98.7% (77/78)	98.4% (63/64)	100% (14/14)
Sensitivity	FP MRA	92.6% (25/27)	91.7% (22/24)	100% (3/3)
	FP + SS MRA	96.3% (26/27)	100% (24/24)	66.7% (2/3)
	CTA	96.3% (26/27)	95.8% (23/24)	100% (3/3)
Specificity	FP MRA	100% (51/51)	100% (40/40)	100% (11/11)
	FP + SS MRA	98.0% (50/51)	97.5% (39/40)	100% (11/11)
	CTA	100% (51/51)	100% (40/40)	100% (11/11)
PPV	FP MRA	100% (25/25)	100% (22/22)	100% (3/3)
	FP + SS MRA	96.3% (26/27)	96% (24/25)	100% (2/2)
	CTA	100% (26/26)	100% (23/23)	100% (3/3)
NPV	FP MRA	96.2% (51/53)	95.2% (40/42)	100% (11/11)
	FP + SS MRA	98.0% (50/51)	100% (39/39)	91.7% (11/12)
	CTA	98.1% (51/52)	97.6% (40/41)	100% (11/11)

TABLE 2. Cross Tabulation of Stenosis Grade on DSA Versus FP MRA, FP + SS MRA, and CTA

	Stenosis Grade on DSA					
	I	II	III	IV	V	NO
Stenosis						
I	32/32/32	0/0/0	0/0/0	0/0/0	0/0/0	0/0/0
II	0/0/0	5/5/5	0/0/0	0/0/0	0/0/0	0/0/0
III	0/0/0	0/0/0	14/14/13	1/2/1	0/0/0	0/0/0
IV	0/0/0	0/0/0	0/0/1	24/23/24	0/0/0	0/0/0
V	0/0/0	0/0/0	0/0/0	0/0/0	2/2/2	0/0/0
NO	0/0/0	0/0/0	0/0/0	0/0/0	0/0/0	2/2/2

Values are expressed as number of cases on CTA/FP MRA/FP + SS MRA, respectively.

NO indicates near occlusion.

[92.8%], respectively). Conversely, when the SS images were of excellent or adequate quality the accuracy of the combined FP + SS reading was slightly improved over that of the FP images alone (63/64 [98.4%] vs. 62/64 [96.9%], respectively). Similar overall accuracy to that of the combined FP + SS reading was noted for CTA.

Overestimation of a moderate (grade III) stenosis on DSA as severe (grade IV) occurred in one case during the combined FP + SS MRA reading. Conversely, 2 cases of severe (grade IV) stenosis at DSA were judged as moderate (grade III) during the FP MRA reading compared with only one case during the combined FP + SS MRA reading (Table 2).

McNemar's test revealed no significant differences ($0.5 < P < 0.9$) between FP MRA, FP + SS MRA, and CTA regarding the grading of stenosis. This finding was confirmed by receiver-operator curve analysis (Fig. 1); analysis of the area under the respective curves revealed no significant difference between the 3 modalities ($P = 0.838$).

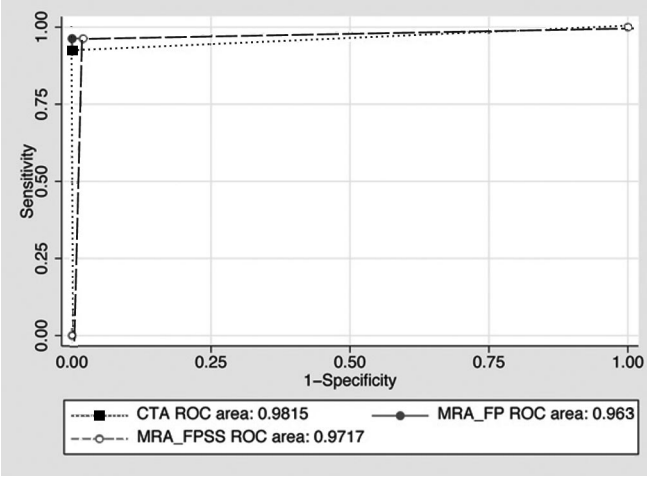

FIGURE 1. ROC analysis for stenosis assessment.

TABLE 3. Diagnostic Performance of FP MRA, FP + SS MRA, and CTA for the Correct Evaluation of Plaque Morphology

		SS Image Quality		
Parameter	**Image Set**	**All (n = 78)**	**Adequate/ Excellent (n = 64)**	**Poor (n = 14)**
Accuracy	FP MRA	83.3% (65/78)	81.3% (52/64)	92.9% (13/14)
	FP + SS MRA	96.1% (75/78)	96.9% (62/64)	92.9% (13/14)
	CTA	98.7% (77/78)	98.4% (63/64)	100% (14/14)
Sensitivity	FP MRA	81.6% (40/49)	80% (36/45)	100% (4/4)
	FP + SS MRA	95.9% (47/49)	97.8% (44/45)	100% (4/4)
	CTA	97.9% (48/49)	97.8% (44/45)	100% (4/4)
Specificity	FP MRA	86.2% (25/29)	84.2% (16/19)	90% (9/10)
	FP + SS MRA	96.6% (28/29)	94.7% (18/19)	90% (9/10)
	CTA	100% (29/29)	100% (19/19)	100% (10/10)
PPV	FP MRA	90.9% (40/44)	92.3% (36/39)	80% (4/5)
	FP + SS MRA	97.9% (47/48)	97.8% (44/45)	80% (4/5)
	CTA	100% (48/48)	100% (44/44)	100% (4/4)
NPV	FP MRA	73.5% (25/34)	64% (16/25)	100% (9/9)
	FP + SS MRA	93.3% (28/30)	94.7% (18/19)	100% (9/9)
	CTA	96.7% (29/30)	95% (19/20)	100% (10/10)

TABLE 4. Diagnostic Performance of FP MRA, FP + SS MRA, and CTA for the Correct Depiction of Ulcerations

		SS Image Quality		
Parameter	**Image Set**	**All (n = 78)**	**Adequate/ Excellent (n = 64)**	**Poor (n = 14)**
Accuracy	FP MRA	87.2% (68/78)	85.9% (55/64)	92.9% (13/14)
	FP + SS MRA	97.4% (76/78)	98.4% (63/64)	92.9% (13/14)
	CTA	98.7% (77/78)	98.4% (63/64)	100% (14/14)
Sensitivity	FP MRA	85.4% (41/48)	84.1% (37/44)	100% (4/4)
	FP + SS MRA	97.9% (47/48)	97.7% (43/44)	100% (4/4)
	CTA	97.9% (47/48)	97.7% (43/44)	100% (4/4)
Specificity	FP MRA	90% (27/30)	90% (18/20)	90% (9/10)
	FP + SS MRA	96.7% (29/30)	100% (20/20)	90% (9/10)
	CTA	100% (30/30)	100% (20/20)	100% (10/10)
PPV	FP MRA	93.2% (41/44)	94.9% (37/39)	80% (4/5)
	FP + SS MRA	97.9% (47/48)	100% (43/43)	80% (4/5)
	CTA	100% (47/47)	100% (43/43)	100% (4/4)
NPV	FP MRA	79.4% (27/34)	72% (18/25)	100% (9/9)
	FP + SS MRA	96.7% (29/30)	95.2% (20/21)	100% (9/9)
	CTA	96.7% (30/31)	95.2% (20/21)	100% (10/10)

TABLE 5. Cross Tabulation of Plaque Morphology and Ulceration on DSA Versus FP MRA, FP + SS MRA, and CTA Acquisitions

	DSA	
	Regular	**Irregular**
Plaque morphology		
Regular	25/28/29	9/2/1
Irregular	4/1/0	40/47/48
	Ulcerated	**Not ulcerated**
Ulcerations		
Ulcerated	41/47/47	3/1/0
Not ulcerated	7/1/1	27/29/30

Values represent findings for FP MRA, FP + SS MRA, and CTA.

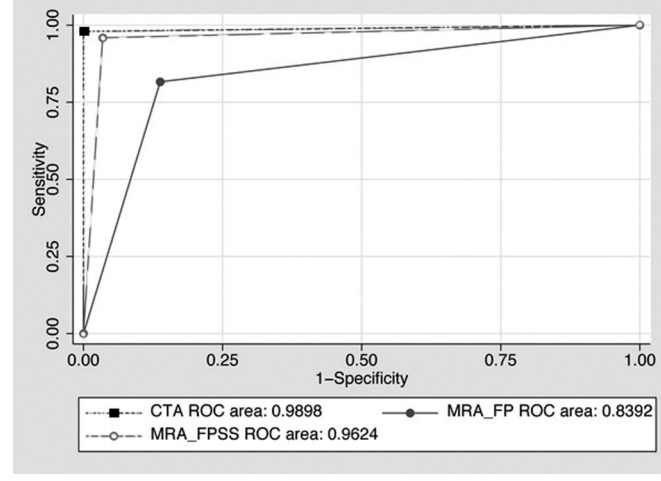

FIGURE 2. ROC analysis for plaque morphology assessment.

Plaque Morphology, Plaque Length, and Tandem Lesions

Inter-reader agreement was very good for all modalities for evaluations of plaque morphology ($0.87 < \kappa < 0.93$), stenosis length ($0.88 < \kappa < 0.96$), and tandem lesions ($0.85 < \kappa < 0.95$). Diagnostic performance for the correct evaluation of plaque morphology and ulcerations is presented in Tables 3 and 4, respectively. Superior accuracy was apparent for combined FP + SS MRA compared with FP MRA for both the evaluation of plaque morphology (96.1% vs. 83.3%) and the depiction of ulcers (97.4% vs. 87.2%), reflecting the higher spatial resolution achievable on SS imaging. The corresponding accuracy on CTA was 98.7% for both evaluations. Vascular irregularities or ulcerations were missed (ie, false negative findings) in 9 and 7 cases, respectively, at FP MRA but only in 2 and 1 cases at combined evaluation of FP + SS MRA images. Conversely, CTA missed 1 vascular irregularity and 1 ulceration (Table 5). Likewise, false positive reports of ulceration were noted at FP MRA in 3 cases, at combined FP + SS MRA in 1 case but in no case at CTA.

Both McNemar's test and area under the curve analysis revealed significant differences between the 3 modalities in terms of plaque morphology evaluation ($P = 0.001$; Fig. 2) and ulcer depiction ($P = 0.01$; Fig. 3). No significant differences were noted for the evaluation of plaque length and tandem lesions ($P = 1$; all evaluations).

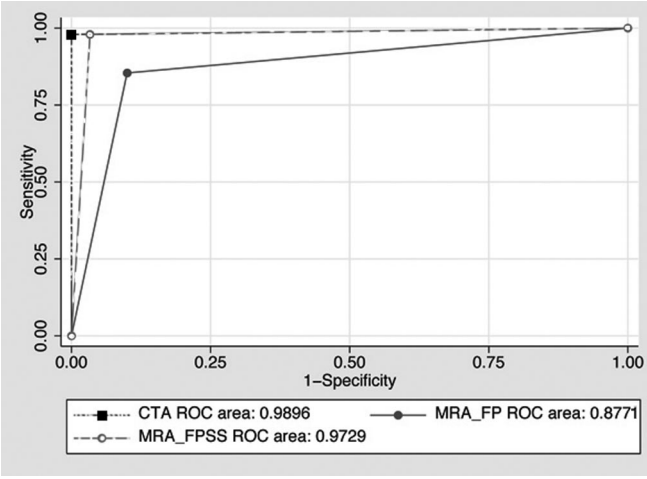

FIGURE 3. ROC analysis for depiction of ulcerations.

Impact on Diagnosis

The 14 of 80 (17.5%) vessels whose SS image quality was rated poor were each nondiagnostic and scored as −1 for impact on final diagnosis as compared with DSA. Additional SS images did not provide any diagnostic benefit (Fig. 4) for a further 9 (11.3% overall) vessels (scored as 0) but led to increased diagnostic confidence (Fig. 5) for 49 (61.3% overall) vessels (scored as 1). Additional SS images of the remaining 8 (10% overall) vessels were considered to have a direct positive impact on final diagnosis (scored as 2). In 2 cases the degree of stenosis was initially underestimated on FP images (Fig. 6) whereas in 6 cases small vascular wall irregularities (Fig. 7) or ulcerations (Fig. 8) of the plaque surface were identified only after reading the SS images. Spearman's correlation coefficient revealed good correlation between excellent/adequate SS image quality and impact on final diagnosis ($R(s) = 0.7$; $P < 0.0001$).

DISCUSSION

A major advantage of MRA for noninvasive vascular imaging is the absence of ionizing radiation. However, in the absence of advanced scanner technology (high-performance gradient systems, parallel imaging, and high parallel-imaging acceleration factors, improved surface coil design) this technique has tended to suffer from lower spatial resolution for routine clinical examinations. The availability of dedicated intravascular "blood pool" contrast agents potentially offers a means to overcome the drawback of reduced spatial resolution by allowing submillimeter isotropic image acquisition without temporal constraints.[25] Unfortunately, the relatively high cost and limited overall applicability beyond vascular imaging are limitations to the widespread use of intravascular agents, particularly when compared with the relative ease of use, robustness, speed, and accuracy of CTA.

Like the intravascular agent gadofosveset,[26,27] gadobenate dimeglumine differs from conventional gadolinium contrast agents because the contrast effective molecule (Gd-BOPTA) interacts with serum albumin.[12–14] These interactions result in a slowing of the tumbling rate of the Gd-BOPTA complex in blood, leading to a longer rotational correlation time with inner shell water protons[28] and hence a reduction of the T1 relaxation time and an increase of the R1 relaxivity compared with other agents at equivalent dose.[11,12] Although the interactions between gadobenate dimeglumine and serum albumin are weaker and more transient than those of gadofosveset,[26,27] and despite pharmacokinetic and elimination profiles that are indistinguishable from those of conventional gadolinium

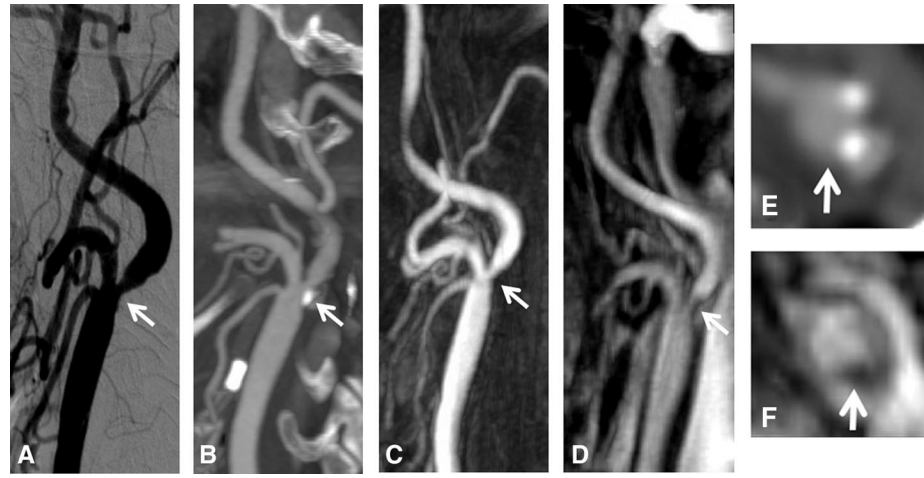

FIGURE 4. DSA (A) reveals a stenosis (NASCET grade II) of the left ICA with long and substantially smooth plaque (arrows). Accurate grading of stenosis was achieved on CTA (B) as well as on CE-MRA FP (C) and SS images (D) with adequate visualization of vessel lumen and walls on all modalities. Coaxial reformations from CTA (E) and SS MRA (F) reveal a plaque at the bifurcation (arrows). In this case the readers assigned a score of zero for the usefulness of the SS acquisition (SS images provide no additional benefit over FP images and have no effect on final diagnosis).

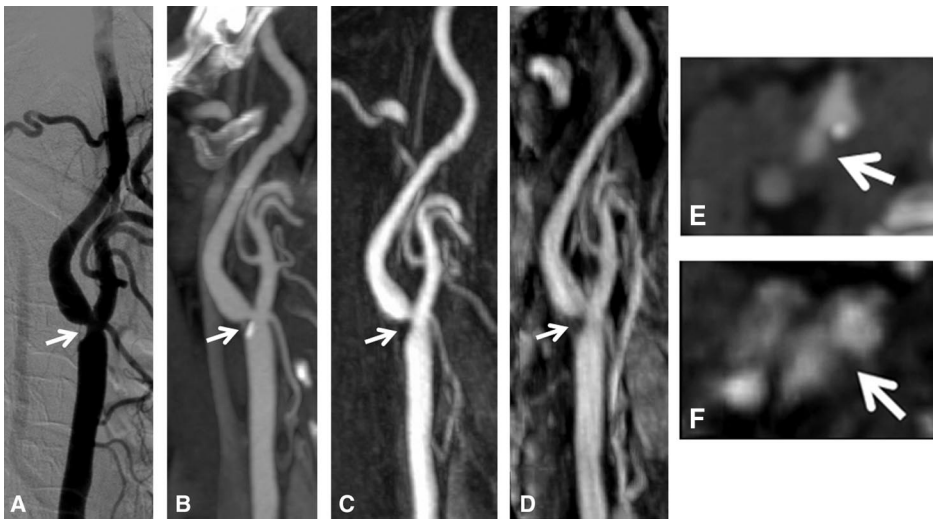

FIGURE 5. DSA (A) reveals narrowing of the lumen (NASCET grade III) of the right ICA because of a focal stenosis caused by a smooth plaque (arrows). Stenosis grading was correctly reported on CTA (B), as well as on CE-MRA FP (C) and SS (D) images. Coaxial reformations from CTA (E) and SS MRA (F) show the lumen at the point of maximum stenosis (arrows). In this case the readers assigned a score of 1 for the usefulness of the SS acquisition (SS images provide similar information to FP images enabling increased confidence).

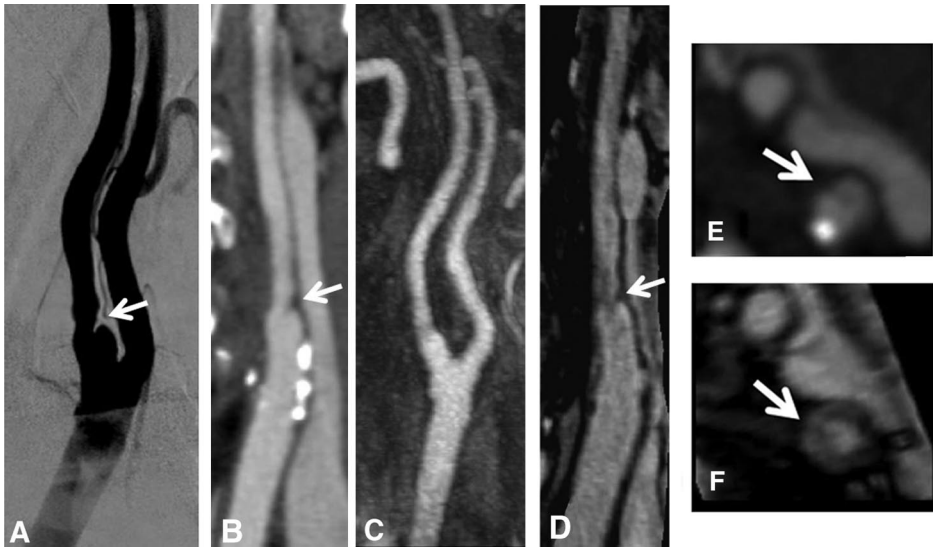

FIGURE 6. DSA (A) reveals an ulcerated plaque causing a NASCET grade II stenosis (arrows) of the left ICA. Stenosis was also reported as grade II at CTA (B), although the ulceration was barely visible. On CE-MRA FP (C) images neither the stenosis nor the ulceration was apparent. The stenosis was correctly graded at SS c-MPR (D) and the ulceration was reported in agreement with DSA. Coaxial reformations from CTA (E) and SS MRA (F) show the lumen at the point of maximum stenosis (arrows). In this case the readers assigned a score of 2 for the usefulness of the SS acquisition (SS images provide additional diagnostic information over FP images potentially or definitely impacting the final diagnosis).

agents,[5] the results of this study suggest that the increased R1 relaxivity of gadobenate dimeglumine is nevertheless still sufficient to permit reliable acquisition of SS images of the carotid vasculature subsequent to routine FP image acquisition. Specifically, our study shows that SS imaging of the carotid arteries with gadobenate dimeglumine is not only feasible but that the information obtained is in most cases complementary to that obtained on FP images and in some cases beneficial for patient diagnosis.

To note is that the acquisition of gadobenate dimeglumine-enhanced SS images in this study occurred within a 4-minute timeframe immediately after completion of FP image acquisition rather than at 5 to 15 minutes after contrast injection as reported for gadofosvest.[3,4] Whereas the temporal acquisition window reflects the elimination profile of gadobenate dimeglumine and the need to acquire images before the enhanced vascular signal is lost, the possibility to obtain SS images over an extended 4-minute period reflects both the elevated R1 relaxivity of gadobenate dimeglumine and, to a lesser extent, the recirculation of contrast agent after the FP. The net result in this study following FP image acquisition was the acquisition of high resolution SS images that were of excellent or adequate quality for 66 of 80 (82.5%) carotid arteries (46 [57.5%] excellent; 20 adequate [25%]) in less than 5 minutes of total magnet time after contrast injection. Importantly, the additional time needed for evaluation of the combined FP + SS image set was little more than that needed for evaluation of the FP images alone (9 ± 3 minutes compared with 5 ± 1 minute).

Although no significant difference in overall accuracy was noted between CE-MRA FP images, CE-MRA FP + SS images, and CTA images based on area under the curve analysis ($P = 0.838$), a tendency for better overall accuracy was noted on combined FP + SS MRA images compared with FP MRA images alone when the SS images were of excellent or adequate quality (98.4% vs. 96.9%, respectively, with only 1 case of underestimation of severe stenosis on FP + SS images). This was the same as that achieved on CTA (98.4%) possibly reflecting the similar spatial resolution of the CE-MRA SS and CTA images in this study. To confirm the additional value of SS acquisitions, the 3 readers reported increased diagnostic confidence for 49 of 80 (61.3%) vessels and a positive impact on final diagnosis for 8 of 80 (10%) vessels. As shown by Spearman's correlation coefficient (R(s) = 0.7; $P = 0.0001$), a

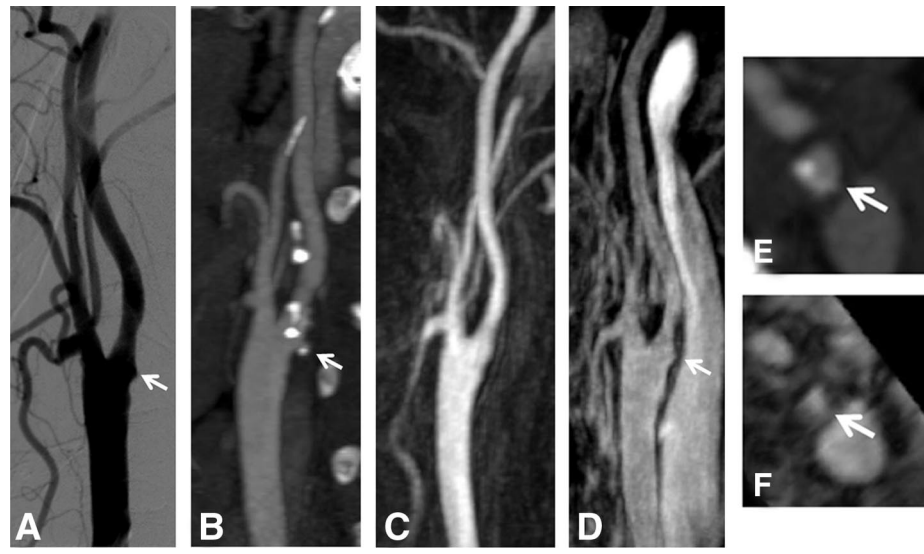

FIGURE 7. DSA (A) reveals a mild (NASCET grade I) stenosis of the left ICA with a deep irregularity of the plaque surface (arrows). Similar features were noted on CTA (B) but not on the CE-MRA FP acquisition (C). The SS MRA acquisition (D), however, confirmed the DSA and CTA findings. Coaxial reformations from CTA (E) and SS MRA (F) reveal subtle plaque irregularities. In this case the readers assigned a score of 2 for the usefulness of the SS acquisition (SS images provide additional diagnostic information over FP images potentially or definitely impacting the final diagnosis).

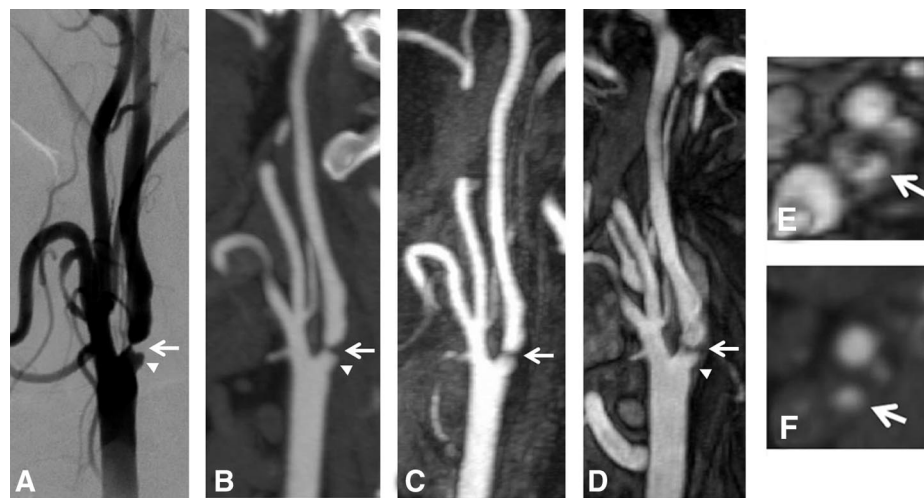

FIGURE 8. DSA (A) reveals a NASCET grade IV stenosis of the left ICA (arrows) with a deep ulceration of the plaque (arrowheads). Both findings are confirmed at CTA (B). The CE-MRA FP acquisition (C) correctly demonstrates the stenosis but fails to show the ulcer. The niche and its margins are, however, well defined on the SS MRA acquisition (D). Coaxial reformations from SS MRA (E) and CTA (F) show residual lumen (arrows). In this case the readers assigned a score of 2 for the usefulness of the SS acquisition (SS images provide additional diagnostic information over FP images potentially or definitely impacting the final diagnosis).

significant correlation was noted between excellent/adequate SS image quality and overall impact on final diagnosis.

Interestingly, all vessels with poor quality at FP imaging (n = 6) were scored as adequate at SS imaging whereas poor vessels at SS imaging (n = 14) were each scored as adequate or excellent at FP imaging. As a result diagnostic quality was achieved for all of the evaluated arteries in the present study. Concerning the poor quality of 6 vessels at routine FP MRA, this was primarily because of slight acquisition mistiming which may have been due to the fact that acquisition timing was determined using a bolus-tracking technique rather than a more robust test bolus technique.

Although SS imaging is clearly not necessary in all cases, particularly when excellent diagnostic quality is achieved at FP imaging, our findings highlight not only the potential of high resolution SS imaging with gadobenate dimeglumine to enhance diagnostic performance even when conventional FP acquisitions are of adequate quality, but suggest also a possible role as a "rescue" technique for routine FP examinations that have failed for technical reasons or otherwise proven nondiagnostic. However, it should be borne in mind that the 4-minute acquisition time limits the applicability of the technique to cooperative patients that are able to remain motionless for the duration of the examination and that the comparatively rapid loss of signal precludes the possibility for repeat SS acquisitions.

As regards the SS imaging protocol, the maximum signal strength of a specific tissue is achieved on 3D GRE sequences when the FA used is that predicted by the Ernst equation (Ernst angle: cos $\alpha_E = \exp(-TR/T1)$). According to this equation higher FA values are to be recommended when the sequence TR values are longer whereas lower FA values should be used when the T1 values are higher. In our study the 30 degree FA was not that predicted by the Ernst equation; based on blood signal-to-noise ratio values alone, a lower FA (theoretically about 17 degrees for a TR of 7.5 milliseconds) should have been used given gadobenate dimeglumine pharmacokinetic data and published in vitro relaxivity data measured at 1.5 T.[12] However, such a small FA may have resulted in reduced contrast between blood and surrounding tissues, most notably the vessel wall. In this regard, it seems the 30 degree FA used in this study was appropriate to maintain sufficient signal-to-noise ratio and blood-tissue contrast throughout the SS acquisition time despite the

progressive reduction in blood signal intensity following the FP acquisition.

In demonstrating the feasibility and diagnostic utility of SS vascular imaging with gadobenate dimeglumine our study fulfils its principal objectives. Nevertheless possible limitations of the study are the relatively small population size and the fact that arbitrary TR and FA values were chosen for SS image acquisition. The evaluation of only 40 patients is perhaps justifiable by the fact that this was a feasibility study to determine the potential of gadobenate dimeglumine as a surrogate intravascular agent. Concerning the selection of arbitrary TR and FA values, this was due to the fact that in vivo studies of blood T1 values after gadobenate dimeglumine administration have yet to be performed. Although direct measurements of the T1 variations in blood and surrounding tissues during the SS image acquisition would allow an analytical a priori optimization of TR and FA, additional studies are necessary to optimize the SS sequence parameters for use with gadobenate dimeglumine. Further work is also warranted to evaluate the potential of gadobenate dimeglumine for SS imaging in other vascular territories such as the peripheral run-off arteries. In this regard, earlier studies have shown that gadobenate dimeglumine is not only effective for conventional FP CE-MRA of the peripheral vasculature[29,30] but that this agent is superior to conventional gadolinium contrast agents at equivalent dose, particularly in the smaller caliper run-off vessels[18,19]; it would be of interest to ascertain whether the greater achievable spatial resolution on SS MRA with gadobenate dimeglumine would improve diagnostic performance still further in this territory.

Concerning the dose of gadobenate dimeglumine administered, a standard volume of 15 mL was used which corresponded to a weight-adjusted dose per patient of between 0.09 and 0.11 mmol/kg bodyweight. Numerous studies with gadobenate dimeglumine have shown that a dose of 0.1 mmol/kg bodyweight is appropriate not only for CE-MRA[18,20–22,29–33] but also for other routine MR imaging applications.[34–41] Given the current widespread concern regarding the use of high doses of gadolinium contrast agents for CE-MRA procedures, particularly in patients with severe renal insufficiency[42–44] the possibility to acquire both FP and SS images with a relatively low dose of gadobenate dimeglumine might be of great interest. To this end it may also be worthwhile investigating the potential for time-resolved carotid MRA with an ultra-low-dose of this agent.[45] Finally, further work is also needed to compare the SS imaging potential of gadobenate dimeglumine directly with that of both intravascular blood-pool agents and conventional gadolinium agents. However, such a comparison was beyond the scope of this preliminary study and should ideally be performed after more complete optimization of the technique.

In conclusion our study demonstrates that high-resolution SS imaging of the carotid arteries with gadobenate dimeglumine is feasible and that the inclusion of an additional 4-minute SS imaging sequence immediately after routine FP imaging can provide additional diagnostic information that is comparable to that available on CTA. Although this preliminary study did not reveal major benefits of FP + SS MRA compared with FP MRA alone regarding the accuracy for detection of clinically relevant stenoses, the results clearly show that SS image acquisition with gadobenate dimeglumine is a viable and effective adjunct procedure for routine clinical use.

REFERENCES

1. Chappell FM, Wardlaw JM, Young GR, et al. Carotid artery stenosis: accuracy of noninvasive tests–individual patient data meta-analysis. *Radiology*. 2009;251:493–502.
2. Hartmann M, Wiethoff AJ, Hentrich HR, et al. Initial imaging recommendations for Vasovist angiography. *Eur Radiol*. 2006;16(suppl 2):B15–B23.
3. Bluemke DA, Stillman AE, Bis KG, et al. Carotid MR angiography: phase II study of safety and efficacy for MS-325. *Radiology*. 2001;219:114–122.
4. Anzidei M, Napoli A, Cavallo Marincola B, et al. Gadofosveset-enhanced MR Angiography of carotid arteries: does steady-state imaging improve accuracy of first-pass imaging? Comparison with selective digital subtraction angiography. *Radiology*. 2009;251:457–466.
5. Spinazzi A, Lorusso V, Pirovano G, et al. Safety, tolerance, biodistribution and MR imaging enhancement of the liver with gadobenate dimeglumine. *Acad Radiol*. 1999;6:282–291.
6. Laurent S, Elst LV, Muller RN. Comparative study of the physicochemical properties of six clinical low molecular weight gadolinium contrast agents. *Contrast Media Mol Imaging*. 2006;1:128–137.
7. Kirchin MA, Runge VM. Contrast agents for magnetic resonance imaging: safety update. *Top Magn Reson Imaging*. 2003;14:426–435.
8. Kirchin MA, Pirovano G, Venetianer C, et al. Safety assessment of gadobenate dimeglumine (Multihance): extended clinical experience from phase I studies to postmarketing surveillance. *J Magn Reson Imaging*. 2001;14:281–294.
9. Shellock FG, Parker JR, Venetianer C, et al. Safety of gadobenate dimeglumine: summary of findings from clinical studies and post-marketing surveillance. *Invest Radiol*. 2006;41:500–509.
10. Shellock FG, Parker JR, Pirovano G, et al. Safety characteristics of gadobenate dimeglumine: clinical experience from intra- and interindividual comparison studies with gadopentetate dimeglumine. *J Magn Reson Imaging*. 2006;24:1378–1385.
11. Rohrer M, Bauer H, Mintorovitch J, et al. Comparison of magnetic properties of MRI contrast media solutions at different magnetic field strengths. *Invest Radiol*. 2005;40:715–724.
12. Pintaske J, Martirosian P, Graf H, et al. Relaxivity of gadopentetate dimeglumine (Magnevist), gadobutrol (Gadovist), and gadobenate dimeglumine (MultiHance) in human blood plasma at 0.2, 1.5, and 3 Tesla [erratum in *Invest Radiol*. 2006;41:859]. *Invest Radiol*. 2006;41:213–221.
13. Giesel FL, von Tengg-Kobligk H, Wilkinson ID, et al. Influence of human serum albumin on longitudinal and transverse relaxation rates (R1 and R2) of magnetic resonance contrast agents. *Invest Radiol.* 2006;41:222–228.
14. Cavagna FM, Maggioni F, Castelli PM, et al. Gadolinium chelates with weak binding to serum proteins. A new class of high-efficiency, general purpose contrast agents for magnetic resonance imaging. *Invest Radiol*. 1997;32:780–796.
15. Bleicher AG, Kanal E. A serial dilution study of gadolinium-based MR imaging agents. *Am J Neuroradiol*. 2008;29:668–673.
16. Yrjänä SK, Vaara T, Karttunen A, et al. Pulse repetition time and contrast enhancement: simulation study of Gd-BOPTA and conventional contrast agent at different field strengths. *Invest Radiol*. 2008;43:267–275.
17. Völk M, Strotzer M, Lenhart M, et al. Renal time-resolved MR angiography: quantitative comparison of gadobenate dimeglumine and gadopentetate dimeglumine with different doses. *Radiology*. 2001;220:484–488.
18. Knopp MV, Giesel FL, von Tengg-Kobligk H, et al. Contrast-enhanced MR angiography of the run-off vasculature: intraindividual comparison of gadobenate dimeglumine with gadopentetate dimeglumine. *J Magn Reson Imaging.* 2003;17:694–702.
19. Wyttenbach R, Gianella S, Alerci M, et al. Prospective Blinded Evaluation of Gd-DOTA– versus Gd-BOPTA–enhanced peripheral MR angiography, as compared with digital subtraction angiography. *Radiology*. 2003;227:261–269.
20. Prokop M, Schneider G, Vanzulli A, et al. Contrast-enhanced MR angiography of the renal arteries: blinded multicenter crossover comparison of gadobenate dimeglumine and gadopentetate dimeglumine. *Radiology*. 2005;234:399–408.
21. Pediconi F, Fraioli F, Catalano C, et al. Gadobenate dimeglumine (Gd-BOPTA) vs. gadopentetate dimeglumine (Gd-DTPA) for contrast-enhanced magnetic resonance angiography (MRA): improvement in intravascular signal intensity and contrast to noise ratio. *Radiol Med (Torino)*. 2003;106:87–93.
22. Bültmann E, Erb G, Kirchin MA, et al. Intra-individual crossover comparison of gadobenate dimeglumine and gadopentetate dimeglumine for contrast-enhanced MR angiography of the supraaortic vessels at 3 Tesla. *Invest Radiol*. 2008;2008:43:695–702.
23. Anzalone N, Scomazzoni F, Castellano R, et al. Carotid artery stenosis: intra-individual correlations of unenhanced MR angiography, and digital subtraction angiography versus rotational angiography for detection and grading. *Radiology*. 2005;236:204–221.

24. North American Symptomatic Carotid Endarterectomy Trial Collaborators. Beneficial effect of carotid endarterectomy in symptomatic patients with high-grade carotid stenosis. *N Engl J Med*. 1991;325:445–453.
25. Nikolaou K, Kramer H, Grosse C, et al. High-spatial-resolution multistation MR angiography with parallel imaging and blood pool contrast agent: initial experience. *Radiology*. 2006;241:861–872.
26. Lauffer RB, Parmelee DJ, Dunham SU, et al. Gadofosveset: albumin-targeted contrast agent for MR angiography. *Radiology*. 1998;207:529–538.
27. Caravan P, Cloutier NJ, Greenfield MT, et al. The interaction of gadofosveset with human serum albumin and its effect on proton relaxation rates. *J Am Chem Soc*. 2002;124:3152–3162.
28. Banci L, Bertini I, Luchinat C. *Nuclear and Electron Relaxation*. Weinheim, Germany: VCH Verlagsgesellschaft GmbH; 1991:138.
29. Thurnher S, Miller S, Schneider G, et al. Diagnostic performance of gadobenate dimeglumine enhanced MR angiography of the iliofemoral and calf arteries: a large-scale multicenter trial. *Am J Roentgenol*. 2007;189:1223–1237.
30. Soulez G, Pasowicz M, Benea G, et al. Renal artery stenosis evaluation: diagnostic performance of gadobenate dimeglumine-enhanced MR angiography–comparison with DSA. *Radiology*. 2008;247:273–285.
31. Schneider G, Ballarati C, Grazioli L, et al. Gadobenate dimeglumine-enhanced MR angiography: diagnostic performance of four doses for detection and grading of carotid, renal, and aorto-iliac stenoses compared to digital subtraction angiography. *J Magn Reson Imaging*. 2007;26:1020–1032.
32. Kroencke TJ, Wasser MN, Pattynama PM, et al. Gadobenate dimeglumine - enhanced magnetic resonance angiography of the abdominal aorta and renal arteries. *Am J Roentgenol*. 2002;179:1573–1582.
33. Wikström J, Wasser MN, Pattynama PM, et al. Gadobenate dimeglumine - enhanced magnetic resonance angiography of the pelvic arteries. *Invest Radiol*. 2003;38:504–515.
34. Maravilla KR, Maldjian JA, Schmalfuss IM, et al. Contrast enhancement of central nervous system lesions: multicenter intraindividual crossover comparative study of two MR contrast agents. *Radiology*. 2006;240:389–400.
35. Rowley HA, Scialfa G, Gao PY, et al. Contrast-enhanced MR imaging of brain lesions: a large-scale intraindividual crossover comparison of gadobenate dimeglumine versus gadodiamide. *Am J Neuroradiol*. 2008;29:1684–1691.
36. Rumboldt Z, Rowley HA, Steinberg F, et al. Multicenter, double-blind, randomized, intra-individual crossover comparison of gadobenate dimeglumine and gadopentetate dimeglumine in MRI of brain tumors at 3 Tesla. *J Magn Reson Imaging*. 2009;29:760–767.
37. Pediconi F, Catalano C, Occhiato R, et al. Breast lesion detection and characterization at contrast-enhanced MR mammography: gadobenate dimeglumine versus gadopentetate dimeglumine. *Radiology*. 2005;237:45–56.
38. Pediconi F, Catalano C, Padula S, et al. Contrast-enhanced MR mammography: improved lesion detection and differentiation with gadobenate dimeglumine. *Am J Roentgenol*. 2008;191:1339–1346.
39. Pediconi F, Catalano C, Roselli A, et al. The challenge of imaging dense breast parenchyma: is magnetic resonance mammography the technique of choice? A comparative study with x-ray mammography and whole-breast ultrasound. *Invest Radiol*. 2009;44:412–421.
40. Balci NC, Inan N, Anik Y, et al. Low-dose gadobenate dimeglumine versus standard-dose gadopentate dimeglumine for delayed contrast-enhanced cardiac magnetic resonance imaging. *Acad Radiol*. 2006;13:833–839.
41. Bauner KU, Reiser MF, Huber AM. Low dose gadobenate dimeglumine for imaging of chronic myocardial infarction in comparison with standard dose gadopentetate dimeglumine. *Invest Radiol*. 2009;44:95–104.
42. Broome DR, Girguis MS, Baron PW, et al. Gadodiamide-associated nephrogenic systemic fibrosis: why radiologists should be concerned. *Am J Roentgenol*. 2007;188:586–592.
43. Sadowski EA, Bennett LK, Chan MR, et al. Nephrogenic systemic fibrosis: risk factors and incidence estimation. *Radiology*. 2007;243:148–157.
44. Dawson P. Nephrogenic systemic fibrosis: possible mechanisms and imaging management strategies. *J Magn Reson Imaging.* 2008;28:797–804.
45. Lohan DG, Tomasian A, Saleh RS, et al. Ultra-low-dose, time-resolved contrast-enhanced magnetic resonance angiography of the carotid arteries at 3.0 tesla. *Invest Radiol.* 2009;44:207–217.